HAL
open science

Experimental Investigation of the Effective Spectrum Bandwidth of the FSO Link with Scintillation

Zahra Nazari Chaleshtori, Gholami Asghar, Zabih Ghassemlooy, Stanislav Zvanovec

To cite this version:

Zahra Nazari Chaleshtori, Gholami Asghar, Zabih Ghassemlooy, Stanislav Zvanovec. Experimental Investigation of the Effective Spectrum Bandwidth of the FSO Link with Scintillation. 1st West Asian Colloquium on Optical Wireless Communications (WACOWC2018), Apr 2018, Isfahan, Iran. hal-02060245

HAL Id: hal-02060245

https://amu.hal.science/hal-02060245v1

Submitted on 7 Mar 2019

HAL is a multi-disciplinary open access archive for the deposit and dissemination of scientific research documents, whether they are published or not. The documents may come from teaching and research institutions in France or abroad, or from public or private research centers.

L'archive ouverte pluridisciplinaire **HAL**, est destinée au dépôt et à la diffusion de documents scientifiques de niveau recherche, publiés ou non, émanant des établissements d'enseignement et de recherche français ou étrangers, des laboratoires publics ou privés.

Experimental Investigation of the Effective Spectrum Bandwidth of the FSO Link with Scintillation

Zahra Nazari Chaleshtori
Dept. of Electromagnetic Field
Czech Technical University in Prague
Prague, Czech Republic, 16627
nazarzah@fel.cvut.cz

Asghar Gholami
Dept. of Electrical and Computer Engineering
Isfahan University of Technology
Isfahan, Iran, 84156-83111
gholami@cc.iut.ac.ir

Zabih Ghassemlooy
Dept. of Engineering and Environment
Northumbria University
Newcastle upon Tyne, UK
z.ghassemlooy@northumbria.ac.uk

Stanislav Zvanovec
Dept. of Electromagnetic Field
Czech Technical University in Prague
Prague, Czech Republic, 16627
xzvanove@fel.cvut.cz

Abstract— **In free space optical (FSO) communications, the link performance is highly dependent on the atmospheric conditions including turbulence, which causes fluctuations in both the intensity and the phase of the received optical wavefront. In this paper, we experimentally investigate the FSO link considering the ambient temperature and the sun irradiation angle parameters. Furthermore, we investigate the scintillation effect on the FSO link in the frequency domain and present temporal spectra of the irradiance fluctuations. It is worth since it can be helpful to compensate the scintillation effect in a FSO link using adaptive optical alignment system. In addition, we show the measured effective spectrum bandwidth of fluctuations in moderate turbulence is less than 250 Hz for a 220 m link length, and evaluate the environmental effects on it under different turbulence conditions.**

Keywords-scintillation; turbulence; refractive index structure parameter; temporal spectra, FSO

I. INTRODUCTION

Increased needs for bandwidth require technology that goes beyond traditional RF links [1]. Free space optical (FSO) communications is a laser-driven wireless technology that proved to be an important alternative to radio frequency (RF) communication [2, 3]. Because of the advantages offered by FSO systems, including huge data rates, license-free spectrum, inherent security, low power consumption and immunity to the electromagnetic interference, interest in FSO communication systems has grown significantly in recent years [4, 5]. Atmospheric factors are the most serious drawback to FSO systems [6]. A FSO link is highly weather dependent and absorption, scattering and atmospheric turbulence are the most important phenomena that affect the FSO link performance [2, 7]. Optical turbulence resulting from small temperature variations gives rise to power fadings. Due to the small index of refraction fluctuations, an optical wave propagating through atmospheric turbulence will experience irradiance fluctuations (called scintillation), which have a strong impact on the FSO link performance by giving rise to both power loss and phase distortions [8]. The refractive index structure parameter C_n^2 as one of the main turbulence measures influence the scintillation strength [8]. We experimentally measured the value of C_n^2 for several days and nights. We also investigated environment parameters that affect the FSO link performance under turbulence. In [9] changes of C_n^2 during the day for different seasons were reported, but authors did not discuss the atmosphere effects on the turbulence and the relationship between the turbulence and the elapsed time after sunrise (i.e., solar hour). Moreover, based on the in-situ macroscale meteorological measurements, an empirical model for estimating C_n^2 as a function of the elapsed time between the sunrise and sunset (i.e., the temporal time) was introduced in [10], where a look-up table was used for the temporal time. The effect of sun irradiation angle parameters on the scintillation is reported in our previous work paper [11].

In [12] the average temporal spectra of the irradiance fluctuations in individual pixels was reported. However, the aforementioned work did not investigate the environmental effects on the temporal spectra of the irradiance fluctuations. Moreover, investigating the received signal in the frequency domain allows us to determine the maximum non-negligible frequency of fluctuations caused by turbulence, which can be beneficial in design and performance evaluation of FSO systems. It is worth so that it may be helpful to compensate the scintillation effect in a FSO link using adaptive optical alignment system. In this paper to obtain the temporal spectra of the irradiance fluctuations, we use Fourier transformations of the received optical signal affected by scintillation and by calculating the average spectra; the effective spectrum bandwidth of fluctuations (ESBF) is presented and several parameters that affect it are investigated. Moreover, we present the normalized received signal and its probability density function (PDF) for two scenarios under different turbulence regimes, and C_n^2 and ESBF variation with respect to the time of day and other key parameters that affect the link performance under turbulence is investigated.

The paper is organized as follows. In Section II, the-scintillation model is presented. In Section III the experimental set-up and in Section IV experimental results are discussed. Finally, Section V concludes the paper with a brief summary.

II. THE TURBULENT ATMOSPHERIC CHANNEL

Solar radiation absorbed by air around the earth surface causes its denseness to be reduced and combined with the higher

altitude air, so this phenomenon induces the air temperature to fluctuate randomly [13, 14]. Inhomogeneities caused by turbulence can be viewed as eddies of different temperature, acting like refractive prisms of different sizes and indices of refraction. Therefore, the atmosphere refractive index will change randomly, which leads to the deflection of the optical beam from its line of sight path, thus resulting in optical intensity fluctuation at the receiver (Rx), which is known as the scintillation. Atmospheric turbulence is a function of the optical path and is classified as weak, moderate, strong and under saturation regimes [15]. To model scintillation, we utilized lognormal distribution, where the PDF of light intensity I is expressed by [15]:

$$P(I) = \frac{1}{I\sigma_I\sqrt{2\pi}} \exp\left(-\left[\ln\left(\frac{I}{Io}\right) + \frac{\sigma_I^2}{2} \right]^2 \Big/ 2\sigma_I^2 \right). \quad (1)$$

where I_o is the intensity in free space without turbulence. The variance of natural logarithm of intensity σ_I^2 is given by [16]:

$$\sigma_I^2 = \exp\left[\frac{0.49\sigma_R^2}{(1+1.11\sigma_R^{12/3})^{7/6}} + \frac{0.51\sigma_R^2}{(1+0.69\sigma_R^{17/5})^{5/6}} \right] - 1. \quad (2)$$

where σ_R^2 is Rytov parameter and is given by [16]:

$$\sigma_R^2 = 1.23 C_n^2 k^{7/6} L^{11/6}. \quad (3)$$

where C_n^2 ($m^{-2/3}$) is the refractive index structure parameter and $k = 2\pi/\lambda$ is the optical wave number and L (m) is the propagation path length, and λ is the wavelength [16].

III. Experimental System

In order to measure atmospheric turbulence parameters evaluate their effects on the FSO link, we developed a dedicated experimental testbed at Isfahan University of Technology, Iran. The schematic experimental set-up of the proposed FSO system is shown in Fig. 1 [11], which is composed of the transmitter (Tx), Rx and atmospheric channel. The FSO link is positioned outdoor for a link span of 220 m and two adjustable mirrors was employed at 110 m away from Tx/Rx modules, which are positioned on an adjustable optical bench located indoor. The Tx uses a pigtailed laser source (LP520-SF15) with an average output power of 10 mW and wavelength of 520 nm and slope efficiency of 0.17 W/A driven with a constant current source. To collimate beam an optical lens with a diameter of 5 cm and focal length of 10 cm was adopted prior to transmission. The Rx consists of a silicon photodetector (PDA10A-EC) with an active area of 1 mm and a responsivity of 0.24 A/W, and an optical lens with a diameter of 5 cm and a focal length of 15 cm. The electrical signal at the output of the photodetector is amplified using a trans-impedance amplifier. To evaluate the irradiance fluctuations (scintillations) we recorded the temporal evolution of the irradiance distribution at a 5 kHz sampling rate in a PC every 5 minutes.

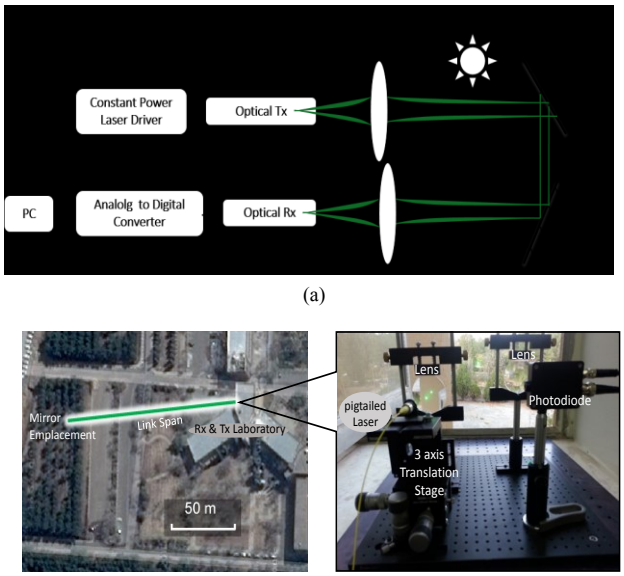

Fig.1. A FSO link: (a) system block diagram, (b) link range, and (c) transmitter and receiver [11]

IV. Experimental Results

To measure the atmospheric turbulence, we calculate the probability distribution of irradiance values, the scintillation index σ_R^2 and then calculate C_n^2 using (3). In addition, the irradiance fluctuations and their temporal spectra were calculated from the recorded data. Here we present the experimental results in two sections (i) C_n^2 with respect to the time of day and night, and the key parameters that affect the FSO link performance; and (ii) the spectrum of the received signal, as well as the effective spectrum bandwidth of fluctuations (ESBF).

A. The C_n^2 parameter

Using the captured data, we first determine the PDF of the atmospheric turbulence and carry out curve fitting with lognormal PDF in order to determine σ_R^2 using (1) and subsequently C_n^2 using (3) for a 220 m link span and λ of 520 nm. The measured data was fitted perfectly with lognormal distribution as R-squared of all data were higher than 0.94. The experimental measurements were taken under the weak to moderate turbulence regimes. Note that, the received values V_{out} were normalized by their respective average $< V_{out} >$ in order to allow for an easier comparison of the curves. Inset in Fig. 2 shows the temporal evolution curves of the irradiance level against time while Fig. 2 depicts the normalized PDF of the signal fitted with a lognormal PDF for σ_R^2 of 0.1818 (i.e., moderate turbulence) and the obtained $C_n^2 = 4.099\times10^{-14}$ $m^{-2/3}$ at time of 13:10.

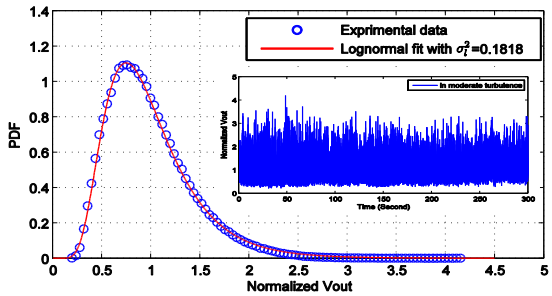

Figure 2. Normalized received signal at the time of 13:10 and the PDF of the received signal fitted with lognormal model for $\sigma_R^2 = 0.1818$

Fig. 3(a) illustrates changes in C_n^2 during the elapsed time between the sunrise and sunset with the ambient temperature T_{am} for 2 Sep. 2015. As can be seen, C_n^2 displays a systematical profile around the noon, increasing after the sunrise reaching its maximum value of ~ 5.3×10^{-14} at noon, where the T_{am} is also at its peak of 31° C, and then decreasing reaching its lowest level at sunset. Note that, changes in the temperature during the noon and the sunset are ~ 5° to 7°. This result illustrates that in addition to T_{am}, the time of day also affects C_n^2 [9].

In order to clarify the relationship between the time of day and C_n^2, we have considered the sun elevation α and declination angles δ. The declination angles δ is the angle between the equator and a line drawn between centers of the earth and the sun, while the elevation angle α represents the angular height of the sun in the sky measured from the horizontal, which varies throughout the day [11]. We determined values for δ and α parameters for each recorded data. Fig. 3(b) depicts the measured C_n^2 and α with respect to the time of the day for 2 Sep. 2015. As shown in Figs. 3(a) and (b), for the same T_{am} values we observed higher scintillation at larger values of α, e.g., for the T_{am} of 28° C and α of 27° and 65° (i.e., at times of 16:15 and 12:00, respectively) the measured C_n^2 are 1.2×10^{-14} $m^{-2/3}$ and 2.3×10^{-14} $m^{-2/3}$, respectively. Our results show that the general pattern of C_n^2 is similar to the results reported in the literature [9, 17]. However, C_n^2 values are different when considering different seasons and the geographic location [11]. So that, larger α and δ angles lead to higher values of C_n^2.

B. *Effective spectral bandwidth of the received signal fluctuations due to beam wandering*

Turbulence in the atmosphere perturbs amplitude and phase of the laser beam wavefront. As a result, temporal and spatial fluctuations of the laser beam intensity (i.e., scintillation) and random changes in beam direction (i.e., beam wandering) or angle-of-arrival fluctuations at the receiver occur, even though the laser transmits a constant wave intensity [1, 2]. Bearing in mind that these fluctuations arise from the slow random changes of atmosphere refractive index, the received optical signal intensity at the receiver surface experiences slow and random variations. Fig. 4 shows V(υ), the normalized spectrum of the received optical signal intensity to its DC spectral component V($\upsilon = 0$). To obtain the temporal spectra of the irradiance fluctuations Fourier transformations are used. As is shown in Fig. 4, the fluctuation spectral energy density has a limited

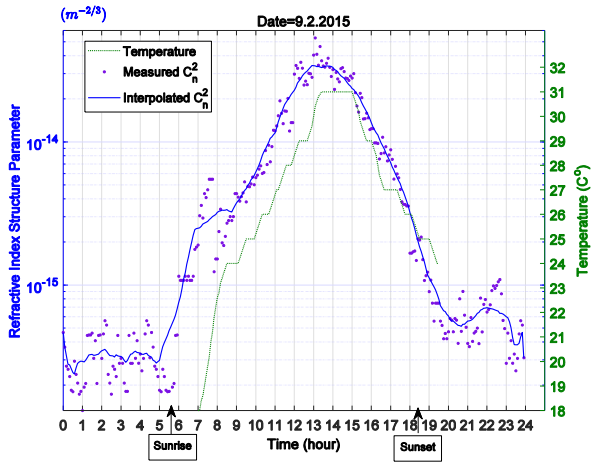

(a)

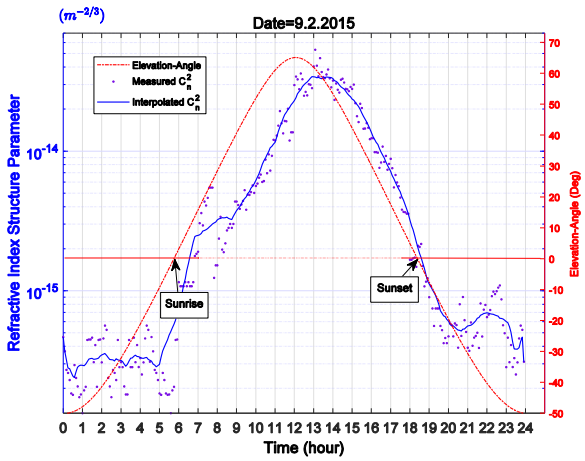

(b)

Figure 3. Changes in C_n^2 versus the time of the day measured on 2 Sep. 2015: (a) with the ambient temperature T_{am}, and (b) with elevation angle.

bandwidth and increasing the frequency, intensity decrease very fast and for some tens of hertz, it is negligible. This means that the fluctuations produced by scintillation are mostly in very low frequencies and for higher frequencies the scintillation effect could be neglected. To quantitate the fluctuation bandwidth, we define a frequency as effective spectrum bandwidth of fluctuations (ESBF) such that the spectral energy density of the fluctuations contains only 0.1% of its total energy for higher than this frequency. ESBF can be easily calculated from the signal's spectral energy density as:

$$\mathrm{R(f)} = \frac{\int_{f}^{+\infty} |V(\upsilon)|^2 \, d\upsilon}{\int_{0}^{+\infty} |V(\upsilon)|^2 \, d\upsilon}, f \geq 0. \tag{4}$$

where $V(\upsilon)$=Fourier$\{v(t)\}$ and $v(t)$ is the received signal sampled for 5 minutes when a CW laser is fed. According to (4), we defined the ESBF where $R(ESBF)$=0.001, ensuring that the energy of fluctuations is negligible for frequencies higher than the ESBF.

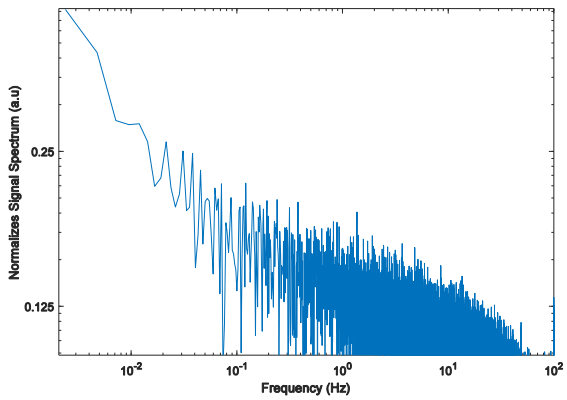

Figure 4. Normalized spectrum of the received signal

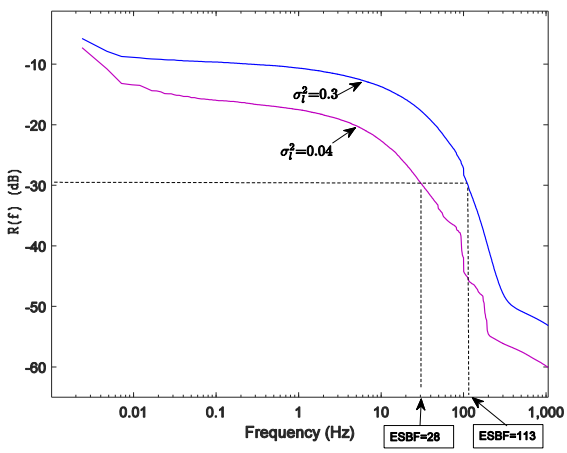

Figure 5. *R*(*f*) and ESBF for two scenarios under different turbulence regimes

Fig. 5 demonstrates the *R*(*f*) and corresponding values of ESBFs for two scenarios under various turbulence regimes. For a turbulence regime with σ_R^2= 0.04 and σ_R^2=0.3, the measured ESBF values are 28 Hz and 113 Hz, respectively. In these measurements the laser source emits a constant optical power.

In Fig. 6 we show the measured C_n^2 and the ESBFs versus the time of the day for 2 Sep. 2015. The measured ESBF for each day are depicted by points and a solid line which interpolates these points. As a result, the ESBF strongly depends on C_n^2.

Figs. 7(a) and (b) show the ESBF versus C_n^2. The measured ESBF corresponding to each C_n^2 is depicted by points. The variation of ESBF versus C_n^2 is interpolated by logarithmic curve, ESBF= $a \log_2(b\ e14\ C_n^2)$ where a , b change with the day of the year. It can be seen that the ESBF increases when scintillation is stronger. According to the experiments, whose results were for weak and moderate turbulence regimes, the ESBFs are less than 250 Hz, see Fig. 7. In this figure for the same value of C_n^2, there are two different values for ESBF in different days. This means that ESBF depends on the other parameters also. To find its dependency, interpolated logarithmic curves from measurement in four different days are compared in Fig. 8. We found that there is a relation between ESBF and the declination angle of the sun (δ). In Fig. 8, for the same C_n^2 values we can observe higher ESBF at larger values of δ, e.g., for $C_n^2 = 1\times10^{-14}$ m$^{-2/3}$ and declination angle of 8.15° and -15.5° the measured ESBF are 110 Hz and 40 Hz, respectively. The results indicate that ESBF depends on both the C_n^2 and δ. An equation representing dependency ESBF on the declination angle δ could be defined in our future works.

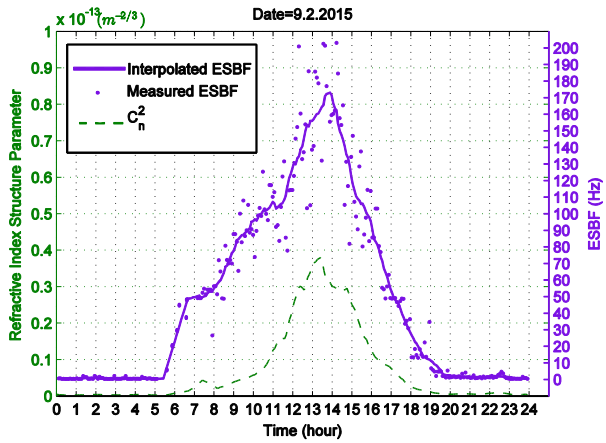

Figure 6. Variation of C_n^2 and measured ESBF versus the time of the day

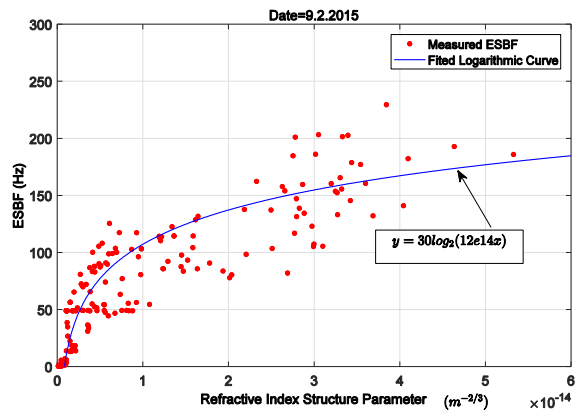

(a)

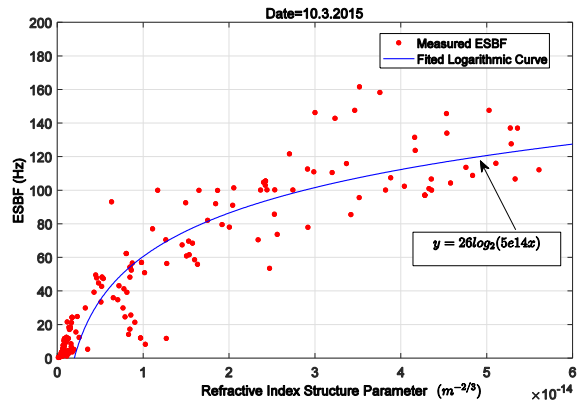

(b)

Figure 7. variation of ESBF versus C_n^2

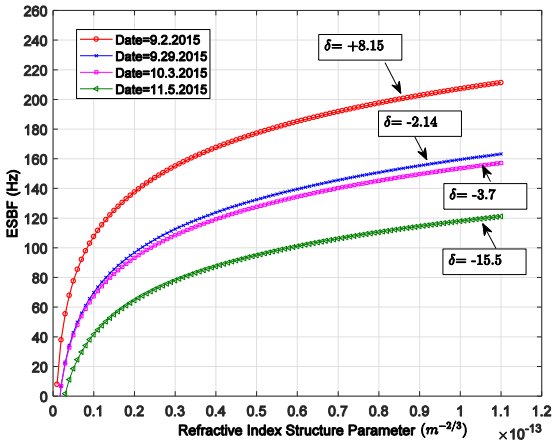

Figure 8. ESBF versus C_n^2 for several days

V. CONCLUSION

In order to investigate the effect of ambient parameters on the scintillation, an experimental link was set up at Isfahan University of Technology. An experimental investigation of scintillation was carried out for the 220 m FSO link for different times of the day and different turbulence conditions. As a demonstrative parameter for the turbulence strength, the refractive index structure parameter C_n^2 was calculated by curve fitting the received signal PDF with a lognormal distribution. In order to clarify the relationship between the time of day and C_n^2, we investigated the sun irradiation angle parameters and showed the dependency of C_n^2 on the time of day, which originally stems from variations of the sun elevation angle. We showed that larger elevation angles resulted in higher intensity fluctuations for a constant temperature. Moreover, we showed that C_n^2 behaved proportionally as an exponential function of α. We have calculated the maximum non-negligible frequency of fluctuations caused by turbulence (i.e., ESBF). According to the experimental results, ESBFs at the measurements were less than 250 Hz for a moderate turbulence regime and a 220 m link span. Furthermore, we deducted that the ESBF increases when scintillation is stronger and its value depends on both the C_n^2 and declination angles δ. This should be investigated in our future works that how the sun location in sky affect ESBF and it could be defined an equation representing dependency ESBF on the declination angle δ.

ACKNOWLEDGMENT

The European project funded by the European Union's Horizon 2020 research and innovation programme under the Marie Slodowska-Curie grant agreement no 764461 (VISION).

REFERENCES

[1] Z. Ghassemlooy, and W. Popoola, *Terrestrial free-space optical communications*. InTech, 2010.

[2] Z. Ghassemlooy, W. Popoola, and S. Rajbhandari, Optical wireless communications: system and channel modelling with Matlab®: CRC Press, 2012

[3] A. Gupta, P. Anand, R. Khajuria, S. Bhagat, and R. K. Jha, "A Survey of Free Space Optical Communication Network Channel over Optical Fiber Cable Communication," International Journal of Computer Applications, vol. 105, pp. 32-36, 2014

[4] K. Li, J. Ma, L. Tan, S. Yu, and C. Zhai, "Performance analysis of fiber-based free-space optical communications with coherent detection spatial diversity," Applied Optics, vol. 55, pp. 4649-4656, 2016.

[5] M. Uysal, C. Capsoni, Z. Ghassemlooy, A. Boucouvalas, and E. Udvary, Optical Wireless Communications: An Emerging Technology: Springer, 2016.

[6] P. Tjondronegoro, "Free-Space Optics for Fixed Wireless Broadband," in Seminar in Communications Engineering, 2004.

[7] A. Vanderka, L. Hajek, J. Latal, J. Vitasek, and P. Koudelka, "Design, Simulation and Testing of the OOK NRZ Modulation Format for Free Space Optic Communication in a Simulation Box," Advances in Electrical and Electronic Engineering, vol. 12, pp. 604-616, 2014.

[8] Andrews, L. C. "Free-space laser propagation: atmospheric effects." In *LEOS Summer Topical Meetings, 2005 Digest of the*, pp. 3-4. IEEE, 2005.

[9] P. Liu, K. Kazaura, K. Wakamori, and M. Matsumoto, "Studies on C 2 n and its effects on free space optical communication system," in Information and Telecommunication Technologies (APSITT), 2010 8th Asia-Pacific Symposium on, 2010, pp. 1-6.

[10] R. Barrios and F. Dios, Wireless optical communications through the turbulent atmosphere: a review: INTECH Open Access Publisher, 2012.

[11] Chaleshtory, Zahra Nazari, Asghar Gholami, Zabih Ghassemlooy, and Mohammad Sedghi. "Experimental Investigation of Environment Effects on the FSO Link With Turbulence." *IEEE Photonics Technology Letters* 29, no. 17, pp.1435-1438, 2017

[12] Weyrauch, T., & Vorontsov, M. A. Free-space laser communications with adaptive optics: Atmospheric compensation experiments. In *Free-Space Laser Communications* (pp. 247-271). Springer, New York, NY. 2004

[13] Popoola, Wasiu Oyewole. "Subcarrier intensity modulated free-space optical communication systems." PhD diss., Northumbria University, 2009.

[14] S. Karp, R. M. Gagliardi, S. E. Moran, and L. B. Stotts, Optical channels: fibers, clouds, water, and the atmosphere: Springer Science & Business Media, 2013.

[15] A. Aladeloba, A. Phillips, and M. Woolfson, "Improved bit error rate evaluation for optically pre-amplified free-space optical communication systems in turbulent atmosphere," IET optoelectronics, vol. 6, pp. 26-33, 2012.

[16] L. C. Andrews, R. L. Phillips, and C. Y. Hopen, Laser beam scintillation with applications vol. 99: SPIE press, 2001.

[17] W. Ni, Y. Miyamoto, K. Wakamori, K. Kazaura, M. Matsumoto, T. Higashino, et al., "Experimental study of atmospheric turbulence effects on RoFSO communication systems," PIERS Online, vol. 5, pp. 65-70, 2009.

View publication stats